JPE 6-2-5

High Efficiency Active Clamp Forward Converter with Synchronous Switch Controlled ZVS Operation

Sung-Sae Lee*, Seong-Wook Choi* and Gun-Woo Moon†

†*Dept. of Electrical Engineering and Computer Science, KAIST, Korea

ABSTRACT

An active clamp ZVS PWM forward converter using a secondary synchronous switch control is proposed in this paper. The proposed converter is suitable for low-voltage and high-current applications. The structure of the proposed converter is the same as a conventional active clamp forward converter. However, since it controls the secondary synchronous switch to build up the primary current during a very short period of time, the ZVS operation is easily achieved without any additional conduction losses of magnetizing current in the transformer and clamp circuit. Furthermore, there are no additional circuits required for the ZVS operation of power switches. Therefore, the proposed converter can achieve high efficiency with low EMI noise, resulting from soft switching without any additional conduction losses, and shows high power density, a result of high efficiency, and requires no additional components. The operational principle and design example are presented. Experimental results demonstrate that the proposed converter can achieve an excellent ZVS performance throughout all load conditions and demonstrates significant improvement in efficiency for the 100W (5V, 20A) prototype converter.

Keywords: DC-DC power conversion, Pulse width modulated power converters, Power distribution

1. Introduction

Recently, many high efficiency and high power density DC/DC power modules have been proposed for distributed power systems servers and telecommunication applications. Among them, the forward converter topology has been widely used for low-voltage and high-current applications with a power level up to 250W. In the conventional forward converter topology[1-2], the power transformer essentially requires a tertiary winding to reset the core. This makes the transformer structure more complicated than that of other single switch converter topologies. Furthermore, the conventional forward topology has another shortcoming; a hard switching operation. Therefore, when the switching frequency is increased to realize small magnetics and capacitors, the overall efficiency will be very low due to increased switching losses. Additionally, high power density is not obtainable due to high cooling requirements. Consequently, the conventional hard switching topology is not suitable for applications in advanced telecommunications and server systems. To solve these problems, soft switching techniques are normally used. Resonant and quasi-resonant converters[3-5] eliminate switching losses by introducing a certain resonance near

Manuscript received September 15, 2005; revised Feb. 23, 2006
†Corresponding Author: gwmoon@ee.kaist.ac.kr
Tel: +82-42-869-3475, Fax: +82-42-861-3475, KAIST
*Dept. of EECS, KAIST, Korea

the switching frequency and allow either the voltage or current to go to zero before the device is turned on and off. While the introduction of resonance allows for zero-current or zero-voltage switching, and therefore enables higher switching frequency, it comes with increased conduction losses and increased stresses on active components when compared with PWM converters. Furthermore, since its output is regulated by frequency modulation, the switching ripples and harmonics vary with the variable switching frequency. Therefore, it becomes very hard to realize the EMC design and compliance. These are the reasons why resonant converters exhibit limited success in improving efficiency and are particularly used for low power applications. In order to achieve a real appreciable efficiency improvement for practical designs, soft switching techniques that eliminate switching losses while preserving minimum voltage and current stresses on switching devices are desired. The active clamp forward converter[6-10] and the forward/flyback converter[2][11] overcome many of the resonant converter's drawbacks. They are operated at a constant frequency and there are no additional current or voltage stresses on active devices while showing good ZVS performance. However these topologies have more increased transformer conduction losses and circulating current losses in the clamp circuit by typically 30-50%, because the small magnetizing inductance is used by the higher magnetizing current to achieve the ZVS operation. This also increases the switch current stresses. The magnetic amplifier can be employed in the secondary side of the active clamp forward or forward/flyback converters to improve the ZVS operation[11][12-13]. However, this method also needs additional components and results in conduction losses in the magnetic amplifier and transformer.

In order to solve all this drawbacks, this paper proposes an active clamp ZVS PWM forward converter using the control of secondary synchronous switch that is suitable for low-voltage and high-current applications. As shown in Fig. 1, the structure of the proposed converter is the same as that of the conventional active clamp forward converter. However, since it controls the secondary synchronous switch to build up the current for the ZVS operation in a very short period of time, the ZVS operation is easily achieved without any additional conduction losses in the transformer and clamp circuit. Furthermore, there are no additional circuits required for the ZVS operation of power switches. Therefore, the proposed converter can achieve high efficiency with low EMI noise resulting from soft switching without any additional conduction losses, and can achieve high power density, a result of high efficiency, and requires no additional components.

The operational principle, design example and experimental results are presented to confirm the validity of the proposed converter.

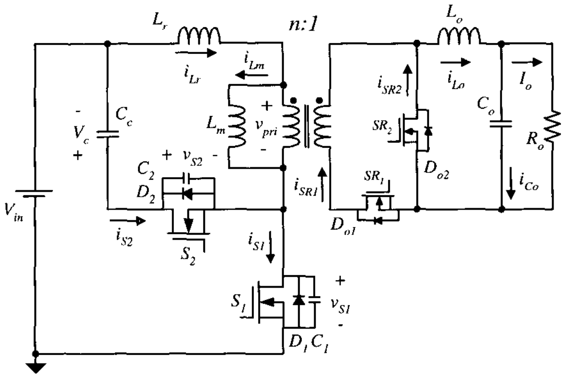

Fig. 1 Circuit diagram of the proposed converter

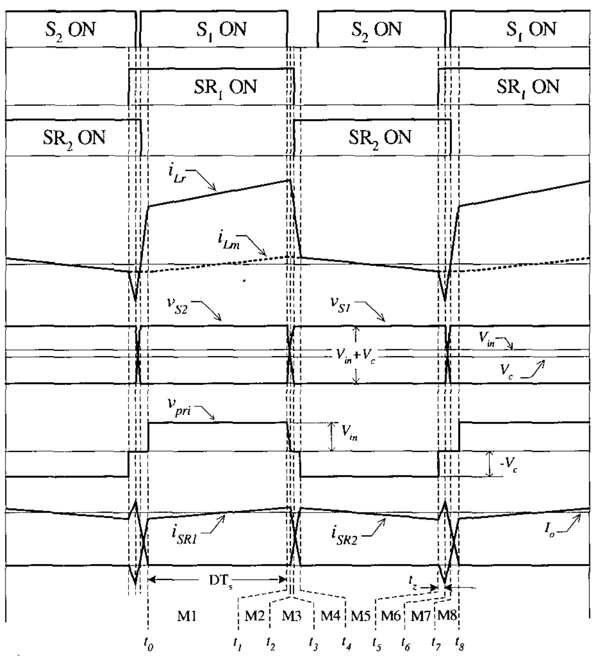

Fig. 2 Key waveforms for the mode analysis

2. Operational Principle

The circuit diagram of the proposed TCB ZVS forward converter is the same as that of the conventional active clamp forward converter as shown in Fig. 1. Switch S_1 is operated in a duty ratio of D, and switch S_2 is operated complementary to S_1 with a time delay between their gate pulses. Synchronous rectifiers are employed instead of Schottky diodes to reduce the conduction loss in the secondary side. Fig. 2 shows the gating pulses for the synchronous switches and key operating waveforms of the proposed converter in the steady state. The gating pulse for SR_1 is imposed before S_2 is turned off. Each switching period is subdivided into eight modes. In order to illustrate the steady state operation, several assumptions are made as follows:

(a) The switches, S_1 and S_2, are ideal except for their internal diode and output capacitor.

(b) The output voltage V_o and clamping capacitor voltage V_c are constant.

(c) The transformer magnetizing current $i_{Lm}(t)$ and leakage inductor current $i_{Lr}(t)$ are constant during the time interval t_1~t_2.

(d) The output capacitors of switches, C_1 and C_2, have the same value of C_s.

Mode 1(t_0~t_1): Mode 1 begins when the commutation of $i_{SR1}(t)$ and $i_{SR2}(t)$ is completed. Then $i_{Lo}(t)$ flows through C_o and SR_1. Since S_1 is on and S_2 is in the off state, V_{in} is applied to L_m+L_r and V_{in}/n-V_o is applied to L_o. Therefore, the power is transferred from the input source to the output. $i_{Lo}(t)$ and $i_{Lr}(t)$ can be expressed as follows:

$$i_{Lo}(t) = \frac{V_{in}/n - V_o}{L_o} t + i_{Lo}(t_0) = i_{SR1}(t) \tag{1}$$

$$i_{Lr}(t) = \frac{V_{in}}{L_m + L_r} t + i_{Lm}(t_0) + \frac{i_{Lo}(t)}{n} = i_{S1}(t) \tag{2}$$

where

$$i_{Lo}(t_0) = I_o - \frac{\Delta i_{Lo}}{2} = I_o - \frac{V_{in}/n - V_o}{2L_o} DT_s$$

$$i_{Lm}(t_0) = -\frac{\Delta i_{Lm}}{2} = -\frac{V_{in}}{2(L_m + L_r)} DT_s .$$

Mode 2(t_1~t_2): This mode begins when S_1 is turned off. Until $v_{S1}(t)$ is lower than V_{in}, the dotted end of the transformer's primary side is positive with respect to the undotted end, while diode D_{o2} is still reversely biased. Therefore, C_1 and C_2 are linearly charged and discharged by $i_{Lr}(t)$, respectively. From this assumption (c), $v_{S1}(t)$ can be expressed as follows:

$$v_{S1}(t) = \frac{i_{Lr}(t_1)}{2C_s} t \tag{3}$$

where

$$i_{Lr}(t_1) = \frac{V_{in}}{2(L_m + L_r)} DT_s + \frac{1}{n}\left(I_o + \frac{V_{in}/n - V_o}{2L_o} DT_s \right).$$

Mode 3(t_2~t_3): After $v_{S1}(t)$ increases to V_{in}, $i_{Lo}(t)$ begins to freewheel through SR_1 and D_{o2}. Since the primary voltage across the transformer is 0V, C_1 and C_2 are charged and discharged in a resonant manner of L_r and C_1+C_2=$2C_s$, respectively. $i_{Lr}(t)$ and $v_{S1}(t)$ can be expressed as follows:

$$i_{Lr}(t) = i_{Lr}(t_2) \cdot \cos\left(\sqrt{\frac{1}{2L_r C_s}}\, t \right) \tag{4}$$

$$v_{S1}(t) = i_{Lr}(t_2) \cdot \sqrt{\frac{L_r}{2C_s}} \cdot \sin\left(\sqrt{\frac{1}{2L_r C_s}}\, t \right) + V_{in} \tag{5}$$

Mode 4(t_3~t_4): After $v_{S1}(t)$ and $v_{S2}(t)$ reach V_{in}+V_c and 0V, respectively, $i_{Lr}(t)$ flows through D_2 and the zero voltage across S_2 is maintained. The ZVS of the SR_2 is guaranteed because the SR_2 is turned on while D_{o2} is conducting. Since D_{o1} and SR_2 are conducting, the voltage across the transformer is 0V and -V_c is all applied to L_r. Therefore, $i_{Lr}(t)$ rapidly decreases as follows:

$$i_{Lr}(t) = -\frac{V_c}{L_r} t + i_{Lr}(t_3) \tag{6}$$

where

$$i_{Lr}(t_3) = \sqrt{ i_{Lr}^2(t_2) - \frac{2C_s V_c^2}{L_r} } .$$

which can be derived form equation (4) and (5).

Mode 5(t_4~t_5): When $i_{Lr}(t)$ reaches $i_{Lm}(t_4)$, $i_{Lo}(t)$ completes its freewheeling and D_{o1} is turned off with D_2 still conducting. Since -V_c is applied to L_m+L_r and -V_o is applied to L_o, $i_{Lo}(t)$ and $i_{Lr}(t)$ can be expressed as follows:

$$i_{Lr}(t) = -\frac{V_c}{L_m + L_r}t + i_{Lm}(t_4) = i_{Lm}(t) \tag{7}$$

$$i_{Lo}(t) = -\frac{V_o}{L_o}t + i_{Lo}(t_4) \tag{8}$$

Since S_2 can be turned on before $i_{Lr}(t)$ decreases to zero, the ZVS operation of S_2 is guaranteed regardless of load variations. In heavy and medium load conditions, the ZVS operation of S_2 can be easily achieved due to a large leakage inductor current at t_2. Furthermore, in the light load conditions, the ZVS operation of S_2 is achieved by a small leakage inductor current at first and then it is achieved by magnetizing current after the end of the secondary inductor current's freewheeling. Therefore, the current build-up that is required for the ZVS operation of S_1 is not required for the ZVS operation of S_2.

Mode 6(t_5~t_6): When SR_1 is turned on while S_2 is in the on state, the transformer secondary voltage becomes zero and therefore the transformer's primary voltage also becomes zero. When transformer's primary voltage becomes zero, $-V_c$ is all applied to L_r. Then $i_{Lr}(t)$ rapidly increases in a negative direction during the very short period of mode. This built-up current is used for the ZVS operation of S_1 in the next mode. Since mode 6 is a very short period of time, the current built-up barely causes additional conduction losses in the primary circuit. $i_{Lr}(t)$ and $i_{SR2}(t)$ can be expressed as follows:

$$i_{Lr}(t) = i_{Lm}(t_5) - \frac{V_c}{L_r}t = -\frac{V_{in}}{2(L_m + L_r)}DT_s - \frac{V_c}{L_r}t \tag{9}$$

$$i_{SR2}(t) = i_{Lo}(t_5) + n \cdot |i_{Lr}(t)|. \tag{10}$$

Mode 7(t_6~t_7): When S_2 is turned off, C_1 and C_2 are discharged and charged, respectively, by $i_{Lr}(t_6)$ in a resonant manner of L_r and $C_1+C_2=2C_s$. Since the leakage inductor current was sufficiently built up to achieve the ZVS operation of S_1 in mode 6, the ZVS operation of S_1 can be easily achieved regardless of load conditions. Fig. 3 shows the different ZVS operations according to different forward converters. In conventional active clamp forward converters[7], the ZVS operation of S_2 is easily achieved due to the large reflected load current or the magnetizing current after the end of the secondary inductor's freewheeling. However, the ZVS operation of S_1 is achieved by the magnetizing current between t_5~t_6 and then it is achieved only by the leakage inductor as shown in Fig. 3(a). Since the leakage inductor has small inductance value, a large current is required to achieve the ZVS operation of S_1. This large current can only be achieved by a large magnetizing current. Therefore, the conventional active clamp forward converter requires a large magnetizing current and transformer conduction loss is inevitable for the ZVS operation of S_1. The active clamp forward converter with the secondary magnetic amplifier [12] can solve this problem as shown in Fig. 3(b). Since the magnetic amplifier prevents the transfer of the magnetizing current to the secondary side, the magnetizing current flows only in the primary winding. Hence, the ZVS operation of S_1 is easily achieved. However, since this converter also requires some magnetizing current, an additional magnetic amplifier and a reset circuit for the magnetic amplifier, the power density is reduced and there exists some conduction loss in the transformer and magnetizing amplifier. Fig. 3(c) shows the ZVS operation of the proposed converter. Since

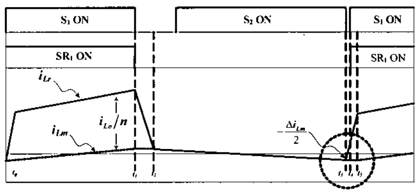

(a) Conventional ACF converter

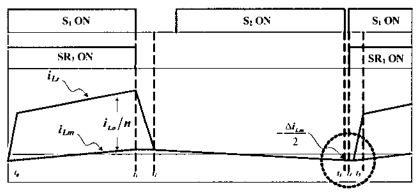

(b) ACF converter with magnetic amplifier

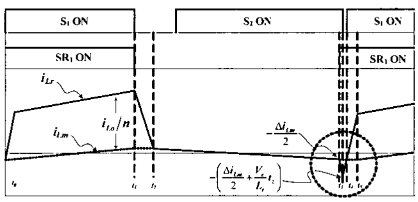

(c) Proposed TCB ZVS ACF converter

Fig. 3 Comparative analysis of the ZVS operation the ZVS current is built up during the very short period of t_5~t_6, the large magnetizing current is not required and the transformer conduction loss can be reduced significantly. Furthermore, no additional circuit is required for the ZVS operation. Therefore, the proposed converter can achieve high efficiency resulting from soft switching without any additional conductional losses in the transformer, and can achieve high power density, a result of high efficiency, without additional components. $i_{Lr}(t)$ and $v_{S2}(t)$ can be expressed as follows:

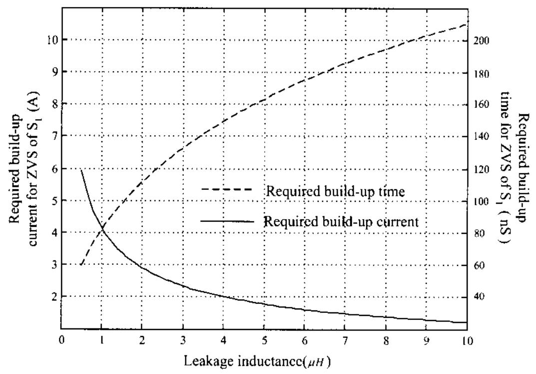

Fig. 4 Required Build-up current and build-up time for ZVS operation

$$i_{Lr}(t) = i_{Lr}(t_6)\cdot\cos\left(\sqrt{\frac{1}{2L_rC_s}}\,t\right) \tag{11}$$

$$v_{S2}(t) = \sqrt{\frac{L_r}{2C_s}}\,i_{Lr}(t_6)\cdot\sin\left(\sqrt{\frac{1}{2L_rC_s}}\,t\right) \tag{12}$$

$i_{Lo}(t)$ begins to freewheel through SR_1 and SR_2 in this mode.

Mode 8(t_7~t_8): After $v_{S1}(t)$ and $v_{S2}(t)$ reach 0V and $V_{in}+V_c$, respectively, S_1 is turned on. Since $i_{Lo}(t)$ is freewheeling through SR_1 and D_{o2}, V_{in} is all applied to L_r. $i_{Lr}(t)$ can be expressed as follows:

$$i_{Lr}(t) = \frac{V_{in}}{L_r}t + i_{Lr}(t_7) \tag{13}$$

where

$$i_{Lr}(t_7) = -\sqrt{i_{Lr}(t_6)^2 - \frac{2C_sV_{in}^2}{L_r}}$$

After the end of mode 8, one switching period is completed and subsequently the operation from t_0 to t_8 is repeated.

3. Design Example

To validate the characteristics of the proposed converter a prototype converter was designed with the following specifications:

- Input voltage V_{in}, 48V DC
- Output voltage Vo, 5V
- Maximum output power Po(max), 100W
- Switching frequency fs, 100kHz
- Maximum duty ratio of S_1, D_{max}, 0.5.

3.1 Selection of turn ratio, n

It is well known that a synchronous switch is used for the output rectifier instead of the Schottky diode, since the Schottky diode has a large forward voltage drop. Assuming that the forward voltage drop caused by the turn-on resistance of the synchronous switch in the secondary side, V_{fd}, is 0.05V (turn-on resistance of IRF3703 is 2.8mΩ) and $D_{max.eff}$=0.45, the turn ratio of the transformer, n, can be derived from the voltage conversion ratio of the conventional active clamp forward converter and can be determined as follows:

$$n = \frac{V_{in}}{(V_o + V_{fd})}D_{max.eff} \tag{14}$$

It is assumed that the current build-up time for the ZVS of S_1(time interval between t_5~t_6) is very short and the effect of the build-up current to voltage conversion ratio is ignored.

3.2 Selection of output inductance, L_o

L_o can be selected by determining the ripple current of the output capacitor. When a continuous conduction mode (CCM) operation is desired until 10% of the full load, L_o can be determined as follows:

$$L_o = \frac{V_o}{\Delta i_{Co}}\left(1 - D_{max.eff}T_s\right) \tag{15}$$

where Δi_{Co} is the ripple current of the output capacitor.

3.3 Selection of magnetizing inductance, L_m

Since the magnetizing current barely affects the ZVS operation in the proposed converter, it is desirable to select the largest possible magnetizing inductance for the transformer. It will not cause any additional conduction losses in the transformer and clamp circuit in the proposed converter.

3.4 Selection of leakage inductance L_r and current build-up time t_z

Since the ZVS operation of S_2 is easily achieved in the active clamp forward converter, L_r should be designed according to the ZVS condition of S_1. From Fig. 3, the ZVS condition of S_1 can be expressed as follows:

$$\frac{1}{2}L_r i_{Lr}(t_6)^2 \geq \frac{1}{2}(2C_s)(V_{in}+V_c)^2 \tag{16}$$

and can be rewritten as follows:

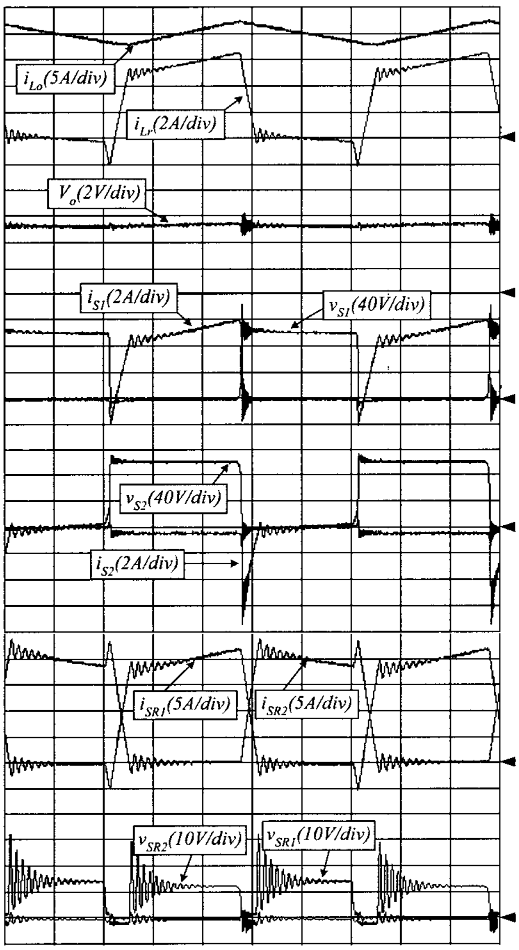

Fig. 5 Key experimental waveforms at full load

$$i_{Lr}(t_6) \geq \sqrt{\frac{2C_s}{L_r}}(V_{in}+V_c) \tag{17}$$

The current build-up time, $t_z=t_6-t_5$, can be expressed as follows:

$$t_z = \frac{L_r}{V_c}\left(i_{Lr}(t_6) - \frac{V_{in}}{2(L_m+L_r)}D_{\max.eff}T_s \right) \tag{18}$$

Fig. 4 plots the required build-up current for the ZVS operation of S_1 with L_r variation and the required current build-up time with the given L_r and build-up current. When a large leakage inductance is selected, a small build-up current is required. However, since this reduces the effective duty and the primary voltage of the transformer during powering, it affects the voltage conversion ratio of the proposed converter. Therefore the leakage inductor value should be selected carefully. Thus, a 4μH was selected in the proposed prototype converter. In this case, the required build-up current for the ZVS of S_1 is 2A and the required build-up time is 150nS with Cs of 1nF.

3. Experimental Results

Based on the design guidelines in the preceding section, a prototype 5V, 100W converter is constructed using the components as shown in Table 1. Fig. 5 shows key waveforms of the proposed converter at full load condition and can be explained as follows:

Table 1 Component list

Switching frequency (f_s)	100kHz
Switches (S_1, S_2)	IRF3315
Synchronous rectifiers (SR_1, SR_2)	IRF3703
Output inductance (L_o)	6 μH
Leakage inductance (L_r)	4 μH
Magnetizing inductance (L_m)	320 μH
Transformer turn ratio (n:1)	4:1
Clamping Capacitance (C_c)	2.2 μF
Output capacitance (C_o)	1000 μF

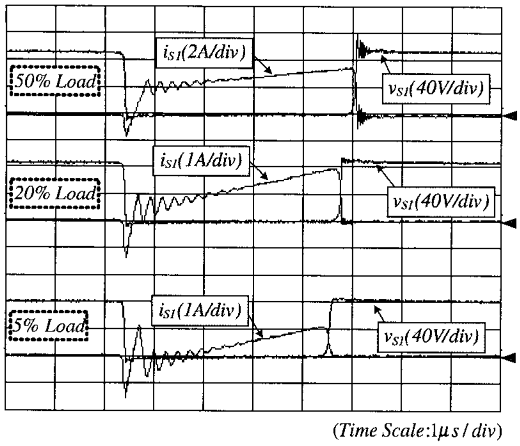

(a) ZVS operation of S_1

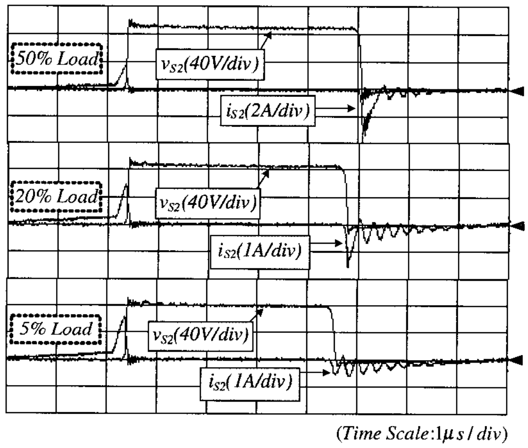

(b) ZVS operation of S_2

Fig. 6 ZVS Operation with load variation

• $i_{Lo}(t)$ has a 4A ripple current as designed in the preceding section. Therefore, the CCM operation is guaranteed until 10% of full load.

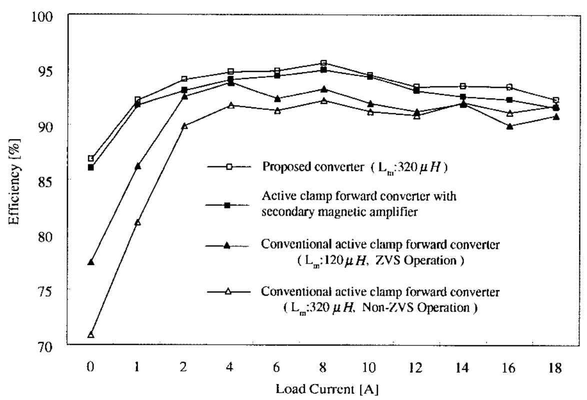

Fig. 7 Efficiency comparison under load variation

• The waveform $i_{Lr}(t)$ is the same as that in conventional active clamp forward converters except for the build-up current before S_2 is turned off. This build-up current is used for the ZVS of S_1. Therefore, a large magnetizing current is not required for the ZVS operation, which is required in the conventional active clamp forward converter.

• The ZVS operation of S_1 is easily achieved due to the build-up current before S_2 is turned off. The ZVS operation of S_2 is also easily achieved as in conventional active clamp forward converters.

• The waveforms of $i_{SR1}(t)$ and $i_{SR2}(t)$ are the same as the theoretic waveforms of Fig. 2. When $i_{Lr}(t)$ is built up, they are negatively and positively increased, respectively.

Fig. 6 shows the voltage and current waveforms of S_1 and S_2, respectively, at different load conditions. As previously mentioned, since the current is built up before S_2 is turned off, the ZVS operation of S_1 is easily achieved regardless of load conditions. The ZVS of S_2 is also easily achieved in the same manner as the conventional active clamp forward converter shown in Fig. 6(b).

Fig. 7 shows the efficiency of the proposed converter, active clamp forward converter with secondary magnetic amplifier and conventional active clamp forward converter with L_m=120μH and L_m=320μH according to load variations. As expected, high efficiency can be obtained around 92% at full load and maximum efficiency occurs at approximately 96%. This high efficiency is the result of reduced switching losses and conduction losses for the entire load ranges by employing the new ZVS scheme of the proposed converter. Therefore, the proposed converter can effectively achieve the ZVS operation of all switches without any additional conduction loss and use of auxiliary circuits.

4. Conclusion

This paper presented the principle of operation, design and experimental results of an active clamp forward converter that uses the control of a synchronous switch for improved ZVS operation. The ZVS operation of S_1 is easily achieved due to the build-up current before S_2 is turned off regardless of load conditions. Furthermore, there are no additional circuits required for ZVS operation. ZVS operation of S_2 is also easily achieved as in conventional active clamp forward converters. Therefore, the proposed converter can achieve high efficiency and low EMI noise resulting from soft switching without any additional conduction losses, and can achieve high power density, a result of high efficiency without additional components. The operational principles were presented in mode analysis with derived design equations. Based on the design equations, a prototype converter was built and tested. The experimental results of the 100W prototype converter prove the key characteristics of the proposed converter. The proposed converter obtained 92% efficiency at full load and maximum efficiency of 96% occurs at around half load. Therefore, the proposed converter is suitable for the power module of servers and telecommunication equipment that require high efficiency, high power density, and low EMI noise with 48V bus voltage.

References

[1] F. D. Tan, " The forward converter: from the classic to the contemporary", IEEE APEC 2002, Vol. 2, 10-14 March 2002, pp. 857-863.

[2] F. D. Tan, " Series of radiation-hardened, high efficiency converters for high voltage bus", IEEE Trans. Aerospace and Electronic Systems, Vol. 38, Issue 4, Oct. 2002, pp. 1324-1334.

[3] K. H. Liu and F. C. Y. Lee, " Zero-voltage switching technique in DC/DC converters", IEEE Trans. Power Electronics, Vol. 5, Issue 3, July 1990, pp., 293-304.

[4] H. J. Kim, C. S. Leu, R. Farrington and F. C. Lee " Clamp mode zero-voltage-switched multi-resonant converters", IEEE PESC, Vol. 1, 29 June-3 July 1992, pp. 78-84.

[5] W. Tang, W. A. Tabisz, A. Lotfi, F. C. Lee and V. Vorperian, "DC analysis and design of forward multi-resonant converter", IEEE PESC, 11-14 June 1990, pp. 862-869.

[6] H. K. Ji and H. J. Kim, "Active clamp forward converter with MOSFET synchronous rectification", in Proc. IEEE PESC, Vol. 2, June 1994, pp. 895-901.

[7] M. Jinno, Jiann-Chem Sheen and Po-Yuan Chen, " Effect of magnetizing inductance on active-clamped forward converters", in Proc. INTELEC, October 2003, pp. 636-642.

[8] D. H. Park, H. J. Kim and Y. S. Sun, " A development of the off-line active clamp ZVS forward converter for telecommunication applications", INTELEC 97, 19-23 Oct. 1997, pp. 271-276.

[9] I. D. Jitaru, " A new high frequency zero-voltage switched PWM converter", IEEE APEC, 23-27 Feb. 1992, pp. 657-664.

[10] J. A. Cobos, O. Garcia, J. Uceda, J. Sebastian and E. de la Cruz, " Comparison of high efficiency low output voltage forward topologies", IEEE PESC, Vol. 2, 20-25 June 1994, pp. 887-894.

[11] I. D. Jitaru, " High frequency, soft transition converters", IEEE APEC, 7-11 March 1993, pp. 880-887.

[12] A. Acik and I. Cadirci, " Active clamped ZVS forward converter with soft-switched synchronous rectifier for high efficiency, low output voltage applications", Electric Power Applications, IEE Proceedings, Vol. 150, Issue 2, March 2003, pp. 165-174.

[13] S. Hamada, H. Ishiwatari, T. Mii and M. Nakaoka, "Saturable reactor & lossless capacitor-assisted soft-switching asymmetrical PWM DC-DC converter with forward-flyback transformer link", IEEE ICON, Vol. 2, 5-10 Aug. 1996, pp. 1011-1016.

Sung-Sae Lee was born in Taegu, Korea, in 1975. He received the B.S. degree in electrical engineering and computer science from Kyungpook National University, Taegu, Korea, in 2001, and the M.S. degree in electrical engineering from Korea Advanced Institute of Science and Technology (KAIST), Daejeon, in 2003, where he is currently pursuing the Ph.D. degree in electrical engineering.

Soeng-Wook Choi was born in Seoul, Korea, in 1975. He received the B.S. degree in electrical engineering from Dankook University, Seoul, Korea, 2002, and the M.S. degree in electrical engineering form Korea Advanced Institute of Science and Technology (KAIST), Daejeon, in 2004, where he is currently pursuing the Ph.D. degree in electrical engineering.

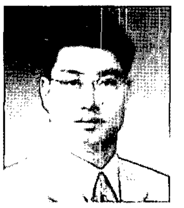

Gun-Woo Moon was born in Korea in 1966. He received the B.S. degree from Han-Yang University, Seoul, Korea, and the M.S. and Ph.D. degrees in Electrical Engineering from the Korea Advanced Institute of Science and Technology (KAIST), Daejeon, in 1990, 1992, and 1996, respectively. He is currently an Associate Professor in the department of Electrical Engineering and Computer Science, KAIST. His research interests include modeling, design and control of power converters, soft-switching power converters, resonant inverters, distributed power systems, power-factor correction, electric drive systems, driver circuits of plasma display panels, and flexible ac transmission systems.

Dr. Moon is a member of the Korean Institute of Power Electronics (KIPE), Korean Institute of Electrical Engineers (KIEE), Korea Institute of Telematics and Electronics (KITE), and Korea Institute of Illumination Electronics and Industrial Equipment (KIIEIE).